Experimental Procedures

Materials

1,2-Distearoyl-sn-glycero-3-phosphoethanolamine-N-[methoxy(poly ethylene glycol)] (DSPE-PEG) was purchased from Avanti Polar Lipids, Inc. DMSO, and other reagents were bought from Sigma-Aldrich. Calcein-AM and PI were obtained from Invitrogen (USA). Phosphate-buffered saline (PBS) (pH 7.4), fetal bovine serum (FBS), DMEM, trypsin-EDTA, and penicillin-streptomycin were purchased from Gibco Life Technologies (AG, Switzerland). All other chemicals used in this study were analytical reagent grade and used without further purification. Ultrapure water (18.25 MΩ.cm, 25 °C) was used to prepare all solutions.

Fabrication of AMQDs

AMQDs were prepared by combining probe and bath sonication liquid phase exfoliation in ethanol. The pulverized antimony (Sb) powder, with initial concentration of 30 mg mL^{-1}, was dispersed in a glass vial containing ethanol. Subsequently, the Sb powder solution was sonicated for 10 h in ice-bath at 500 W with ultrasound probe. The dispersion was allowed to sonicate in an ultrasonic bath for another 6 h at 300 W with an ice-bath. Afterwards, another circle of probe sonication was performed for 5 h in ice-bath at 500 W. The resulting solution was then centrifuged at 3,000 rpm for 20 min. Finally, the supernatant containing AMQDs was collected gently in a clean glass vial for future use.

Surface Modification of AMQDs

To improve the stability of AMQDs in physiological medium, DSPE-PEG was utilized to coat their surface. 10 mg of AMQDs was dispersed in 100 mL chloroform containing pre-dissolved 50 mg DSPE-PEG. After ultra-sonication for 10 min in ice bath, chloroform was removed by vacuum rotary evaporation. The AMQDs-PEG samples were then dissolved in water, centrifuged at 14,000 rpm, and

washed with DI water three times to remove the unbound DSPE-PEG. The final AMQDs-PEG samples were re-suspended in water or PBS, and stored at 4 °C for future use.

Characterization of PEG-coated AMQDs

In our studies, transmission electron microscopy (TEM, JEM-2100UHR, JEOL, Japan) and atomic-force microscopy (AFM, FASTSCANBIO, Germany) were applied to characterize the morphology of the AMQDs both pre- and post-PEG-coating. The chemical compositions of AMQDs and PEG-coated AMQDs were confirmed by Fourier transform infrared spectrophotometer (FT-IR) spectra (Nexus 470, Nicolet, Madison, WI, USA), and X-ray photoelectron spectroscopy (XPS, ESCALAB 250Xi, Japan). X-ray diffraction (XRD, Bruker D8, Germany) and Raman spectrum (HORIBA JOBIN YVON, France) were used to analyze the crystal structure of both coated and uncoated AMQDs. UV-Vis-NIR spectrum was obtained using an Infinite M200 PRO spectrophotometer. The AM concentration was determined by ICP-AES (7000DV, PerkinElmer).

Measurement of photothermal performance

For measuring the photothermal conversion performance of the PEG-coated AMQDs, 1 mL of the PEG-coated AMQD aqueous solutions with various concentrations (0-200 μg mL^{-1}) were placed in a quartz cuvette and exposed to 808 nm NIR laser irradiation at a power density of 1-2 W cm^{-2} for 5 min. The changes in temperature were recorded by an IR thermal camera (TI100 Infrared Camera FLK-TI100 9HZ, FLUKE).

Calculation of extinction coefficiency

The extinction coefficiency of AMQDs and PEG-coated AMQDs was determined according to the Beer-Lambert law. Detailed calculation was as follows:

$$\varepsilon_{808} = \frac{A_{808}}{CL} \quad (1)$$

where ε is the extinction coefficient, A_{808} is the absorption at a wavelength of 808 nm of AMQDs, L is the path length (cm), and C (g L^{-1}) is the weight concentration of the AMQDs or PEG-coated AMQDs. The value of ε of PEG-coated AMQDs was calculated to be 5.58 $Lg^{-1}cm^{-1}$. Although this value is not very high, it is still much higher than some classical PTAs, such as graphene oxide (3.6 $Lg^{-1}cm^{-1}$)[1] and AuNRs (3.9 $Lg^{-1}cm^{-1}$).[2] This strong NIR absorption makes AMQDs promising for cancer PTT.

Calculation of photothermal conversion efficiency (PTCE).

A previously reported method was used to calculate the PTCE of PEG-coated AMQDs. [3] Detailed calculations are as follows:

Based on the total energy balance for this system:

$$\sum_i m_i C_{p,i} \frac{dT}{dt} = Q_{AMQDs} + Q_s - Q_{loss} \quad (2)$$

where m and C_p are the mass and heat capacity of solvent (DI water), respectively. T is the solution temperature.

Q_{AMQDs} is the photothermal energy input by PEG-coated AMQDs:

$$Q_{AMQDs} = I(1 - 10^{-A_{808}})\eta \quad (3)$$

where I is the power of NIR laser, A_{808} is the PEG-coated AMQDs absorbance at 808 nm, and η is the PTCE for the conversion of light to thermal energy.

Q_s is the heat associated with the light absorbance of the solvent.

Q_{loss} is thermal energy lost to the surroundings:

$$Q_{loss} = hA\Delta T \quad (4)$$

where h is the heat transfer coefficient, A is the container surface area, and ΔT is the change in temperature of the solution, which is defined as *T (the solution temp)-*T_{surr} *(the ambient surrounding temp)*

At the maximum steady-state temperature, the heat input is equal to the heat output, that is:

$$Q_{AMQDs} + Q_s = Q_{loss} = hA\Delta T_{max} \quad (5)$$

where ΔT_{max} is the temperature change at the maximum steady-state temperature. According to the Eq.3 and Eq.5, the PTCE (η) can be determined as follows:

$$\eta = \frac{hA\Delta T_{max} - Q_s}{I(1-10^{-A_{808}})} \quad (6)$$

In order to get the *hA*, θ is introduced in, which is defined as the ratio of ΔT to ΔT_{max}:

$$\theta = \frac{\Delta T}{\Delta T_{max}} \quad (7)$$

Substituting Eq.7 into Eq.2 and the rearranging Eq.2 yeilds the new equation:

$$\frac{d\theta}{dt} = \frac{hA}{\sum_i m_i C_{p,i}}\left[\frac{Q_{AMQDs}+Q_s}{hA\Delta T_{max}} - \theta\right] \quad (8)$$

When the laser was shut off, the $Q_{AMQDs}+Q_s = 0$, thus changing Eq.8 to:

$$dt = -\frac{\sum_i m_i C_{p,i}}{hA}\frac{d\theta}{\theta} \quad (9)$$

Integrating Eq.8 gives the expression:

$$t = -\frac{\sum_i m_i C_{p,i}}{hA}\theta \quad (10)$$

Thus, *hA* can be determined by applying the linear time data from the cooling period vs $-\ln\theta$, so that the η of PEG-coated AMQDs can be calculated when the *hA* value is substituted into Eq.6.

Cytotoxicity assay

The viability of cancer cells was evaluated by AlamarBlue assay. First, normal cells HEK293 (a specific cell line originally derived from human embryonic kidney), and various cancer cells (including A549, HeLa, PC3, and MCF-7) were incubated in 96-well plates (5,000 cells/well) with appropriate culture medium at 37 °C in an atmosphere of 5% CO_2 for 24 h. Subsequently, PEG-coated AMQDs with various final concentrations (25-200 μg mL^{-1}) were added to the cells, and allowed to incubate for another 24 h. Lastly, the cells were washed with PBS, and their viabilities were determined by the AlamarBlue assay relative to the control cells (incubated with the same volume of culture medium without adding PEG-coated AMQDs).

***In vitro* photothermal therapy**

MCF-7 and HeLa cells were chosen for evaluation of the photothermal effect of PEG-coated AMQDs. As is routine, MCF-7 and HeLa cells were incubated in 6-well plates at 37 ^{o}C with 5% CO_2 for 24 h. Afterwards, the culture medium was replaced by new medium containing PEG-coated AMQDs at a concentration of 200 μg mL^{-1} for another 4 h. Afterwards, MCF-7 and HeLa treated cells were irradiated with an 808 nm laser at a power density of 1 W cm^{-2} for 5 min. After 3 h incubation , both calcein AM (calcein acetoxymethyl ester) and PI (propidium iodide) were used to co-stain the cells to determine the photothermal effect of PEG-coated AMQDs by a laser scanning confocal microscope.

To quantitatively analyze the photothermal effect of PEG-coated AMQDs, MCF-7 and HeLa cells were plated and incubated in 96-well plates at 37 ^{o}C in an atmosphere of 5% CO_2 and 95% air for 24 h. PEG-coated AMQDs were added with different final concentrations (0-200 μg mL^{-1}), and the cells were allowed to incubate for another 12 h. Subsequently, the cells were exposed to 808 nm NIR laser (1 W cm^{-2}) irradiation for 5 min. Finally, the viability of MCF-7 and HeLa cells was determined by AlamarBlue assay, after incubation for another 24 h.

Animal experiments

Healthy BALB/c normal mice and athymic nude mice (4-5 weeks old) were purchased from Charles River Laboratories. All in vivo studies were performed in accordance with National Institutes of Health animal care guidelines, and in strict pathogen-free conditions in the animal facility of Brigham and Women's Hospital. The animal protocol was approved by the Institutional Animal Care and Use Committees at Harvard Medical School.

Xenograft Tumor model

MCF-7 cells were cultured in DMEM supplemented with 10% FBS at 37 ^{o}C with 5% CO_2. 2×10^6 MCF-7 cells suspended in 100 μL of serum-free cell medium were injected into the right hind leg of

female BALB/c nude mice. The mice were used for further experiments when the tumor had grown to ~100 mm^3.

Pharmacokinetic studies

To study the pharmacokinetic profile *in vivo*, five healthy Balb/c mice were intravenously (i.v.) injected with 100 μL of Cy5.5-PEG-coated AMQDs (1 mg/kg equivalent Cy5.5 for each mouse). At certain time intervals, 20 μL of blood was collected and dissolved in 300 μL of lysis buffer. The concentration of the PEG-coated AMQDs was determined by the fluorescence spectrum. The standard calibration curve was obtained by a series of dilutions. The blank blood sample (without any treatment) was measured to eliminate blood auto-fluorescence during concentration calculation.

Biodistribution analysis

For biodistribution analysis of PEG-coated AMQDs, MCF-7 tumor-bearing female mice were given an i.v. injection of Cy5.5-PEG-coated AMQDs (1 mg/kg equivalent Cy5.5 for each mouse) via tail vein. The major organs (e.g., heart, liver, spleen, lung, and kidney) and tumors were collected, and imaged at 12 h post-injection. The accumulation of PEG-coated AMQDs in major organs and tumors was quantified by detecting the fluorescence intensity (a.u.) of Cy5.5 via Image-J.

***In vivo* photothermal therapy**

To test the photothermal therapeutic effect of PEG-coated AMQDs *in vivo*, MCF-7 tumor-bearing mice were randomly divided into 4 groups (5 mice in each group). G1, G3, and G4 were intratumorly (i.t.) injected with 40 μL saline, 1 mg/mL PEG-coated AMQDs only, and 1 mg/mL PEG-coated AMQDs, respectively. Then the mice in G2 and G4 were anesthetized and irradiated with an 808 nm laser at 1 W cm^{-2} for 10 min. Tumor size and body weight was then measured by calipers and a balance every other day for a period of two weeks. Tumor volume=$4\pi/3\times$(tumor length/2)$\times$(tumor width/2)^2. Relative tumor volumes were calculated as V/V_0, with V_0 being the initial tumor volume at the start of the treatment.

To further confirm their therapeutic effect via direct i.v. injection, five MCF-7 tumor-bearing mice were i.v. injected with 200 μL PEG-coated AMQDs (1.2 mg/mL). After 12 h-post injection, the tumor

sites were irradiated with an 808 nm laser at 2 W cm^{-2} for 10 min. Tumor sizes and body weight were then measured with the same method. Relative tumor volumes were calculated as V/V_0, with V_0 being the initial tumor volume at the start of the treatment.

Hematocylin and eosin (H&E) stained histology

Healthy Balb/c mice were administered with different treatments every 2 days (Group 1: control group without treatment; Group 2: 6 mg/kg PEG-coated AMQDs via intravenous injection; Group 3: 6 mg/kg PEG-coated AMQDs via intratumoral injection; and Group 4: 6 mg/kg PEG-coated AMQDs via oral delivery). After two weeks of treatment, all mice were euthanized and the organs were harvested, fixed in a 10% formalin solution, and embedded in paraffin for H&E staining.

Toxicity assessment of PEG-coated AMQDs *in vivo*

The *in vivo* toxicity of PEG-coated AMQDs was preliminarily evaluated by serum biochemistry and a complete blood panel test. In brief, PEG-coated AMQDs (10 mg/kg) were *i.v.* injected into three groups of healthy Balb/c mice. 1, 7, and 14 days after injection, all five mice in each group were sacrificed to collect blood for serum biochemistry and complete blood panel test. Another five healthy Balb/c mice treated only with PBS were used as controls.

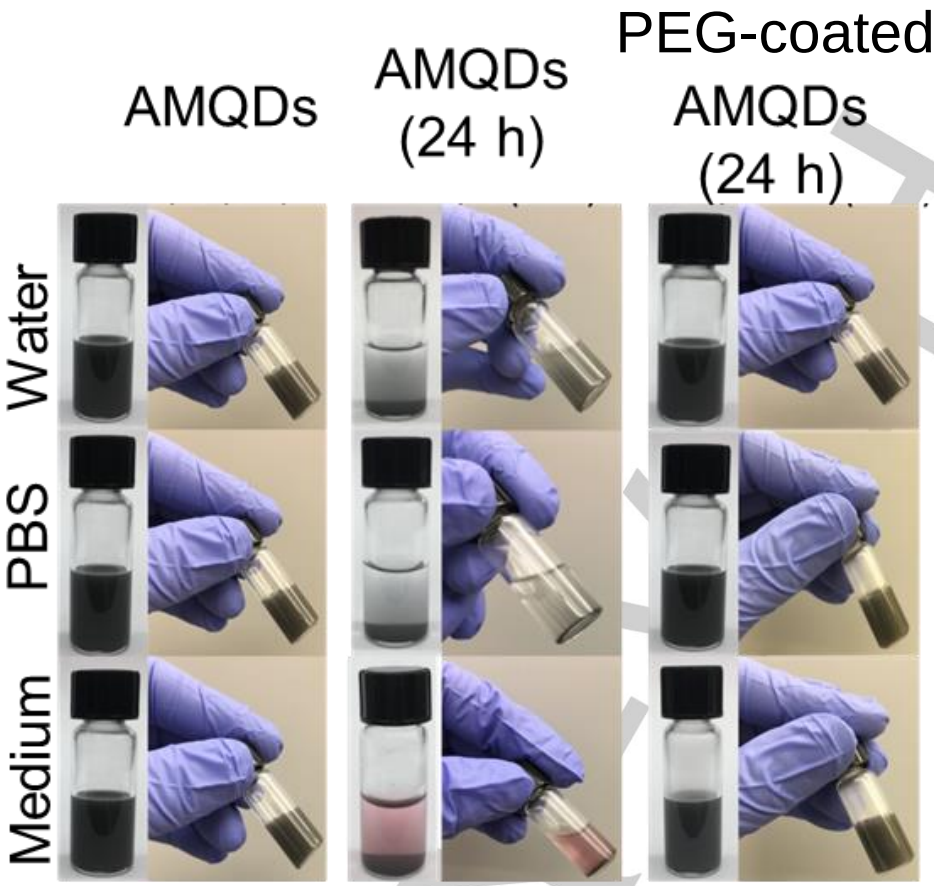

Figure S1. Dispersity of AMQDs and PEG-coated AMQDs in water, PBS, and medium after 24 h incubation.

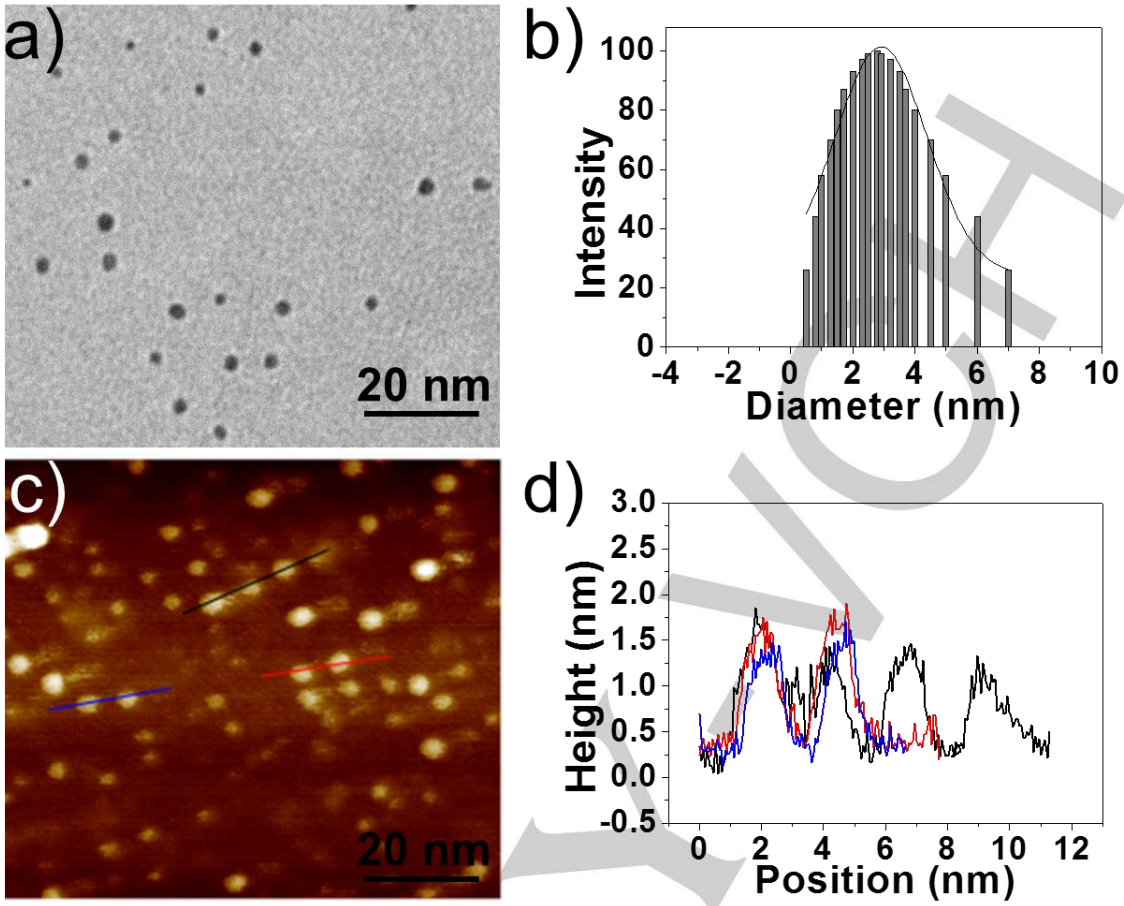

Figure S2. Characterization of as-prepared AMQDs. a) TEM image, c) diameter distribution, b) AFM image, and c) height profile along the lines in d) of the AMQDs.

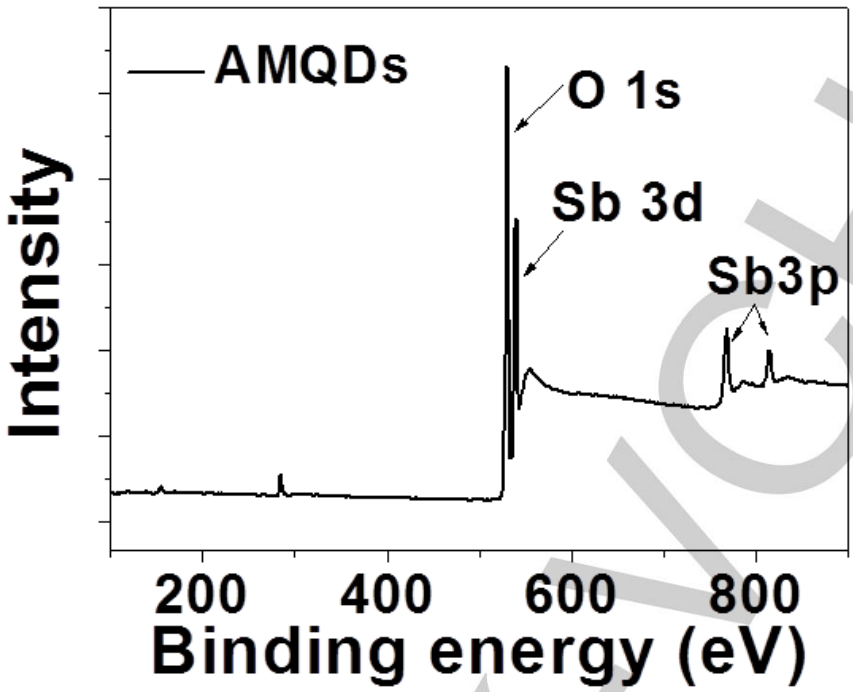

Figure S3. Full scan XPS spectra of as prepared AMQDs.

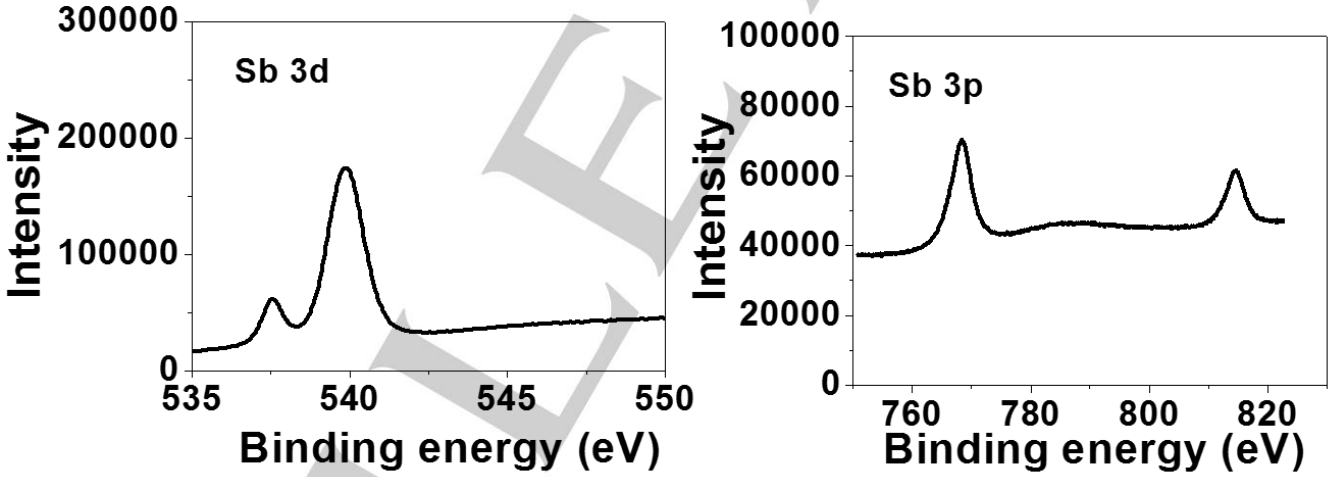

Figure S4. Narrow scan XPS spectra of AMQDs for Sb 3d and Sb 3p.

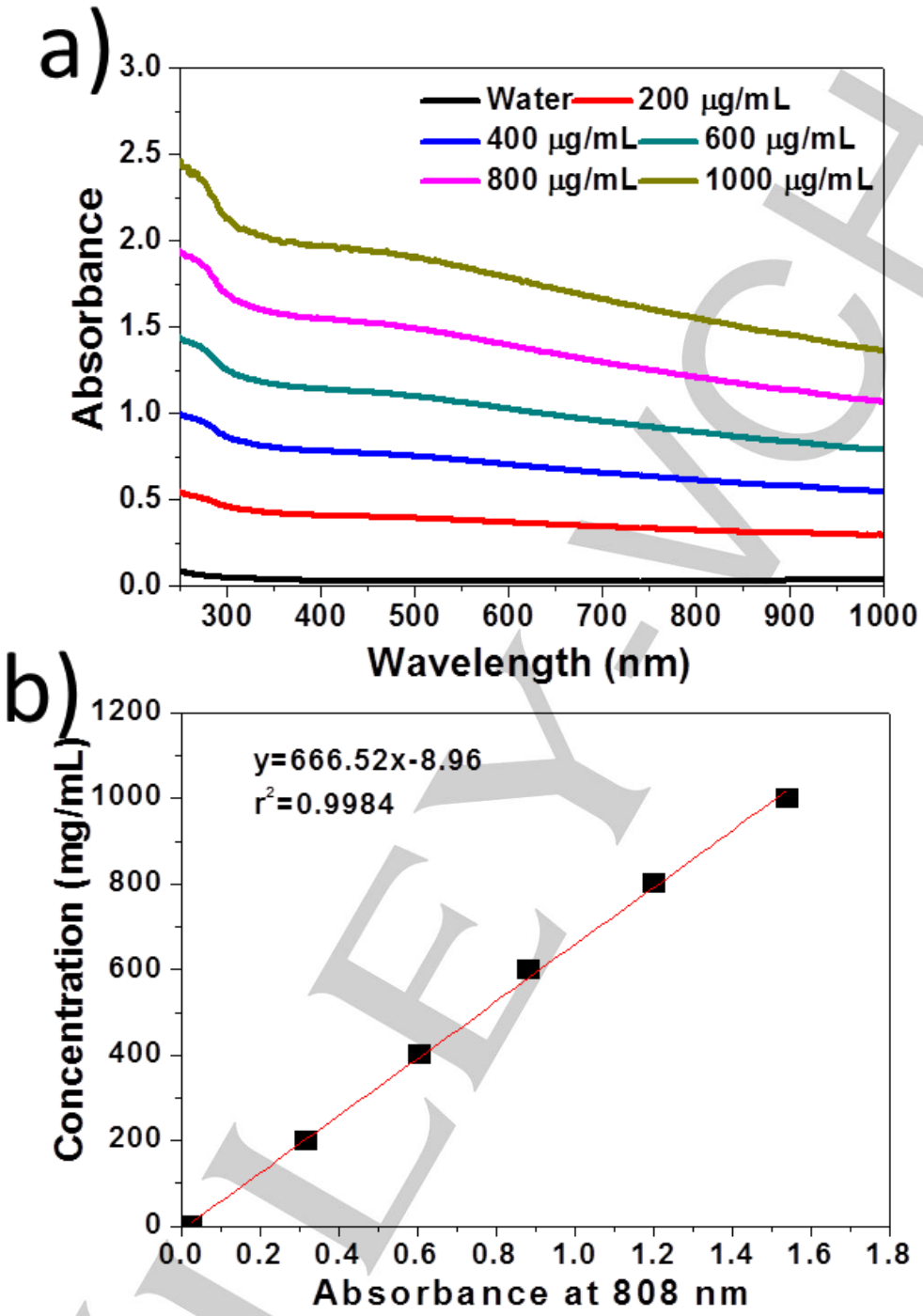

Figure S5. a) Absorbance spectra of AMQDs dispersed in water at different concentrations. b) Normalized absorbance intensity of AMQDs divided by the characteristic length of the cell (A/L) at different concentrations for λ=808 nm.

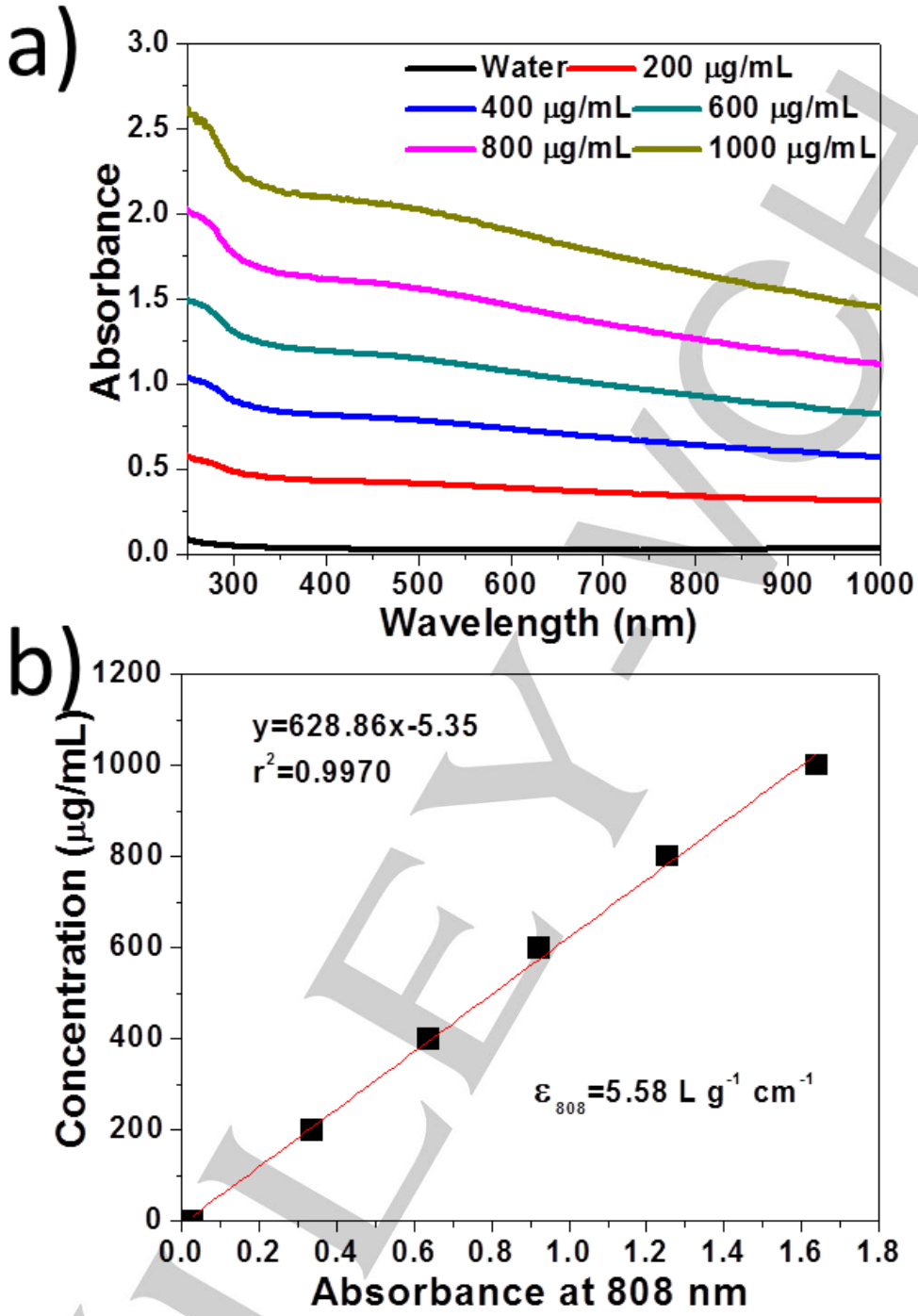

Figure S6. a) Absorbance spectra of PEG-coated AMQDs dispersed in water at different concentrations. b) Normalized absorbance intensity of PEG-coated AMQDs divided by the characteristic length of the cell (A/L) at different concentrations for λ=808 nm. The concentrations are based on AMQDs.

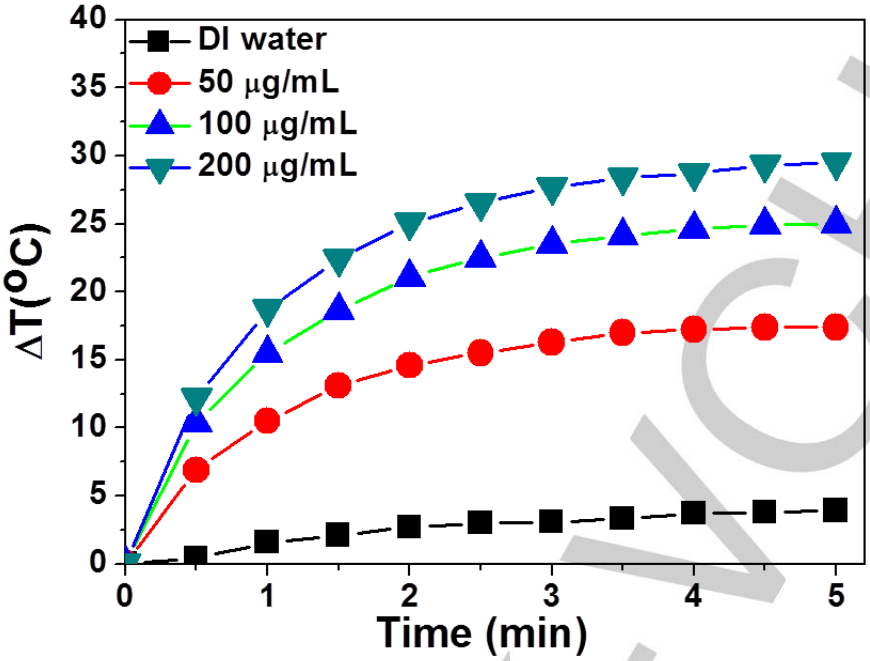

Figure S7. Temperature elevation of water and PEG-coated AMQDs aqueous solutions with different concentrations as a function of time over 5 min irradiation with an NIR laser (808 nm, 1 W cm^{-2}).

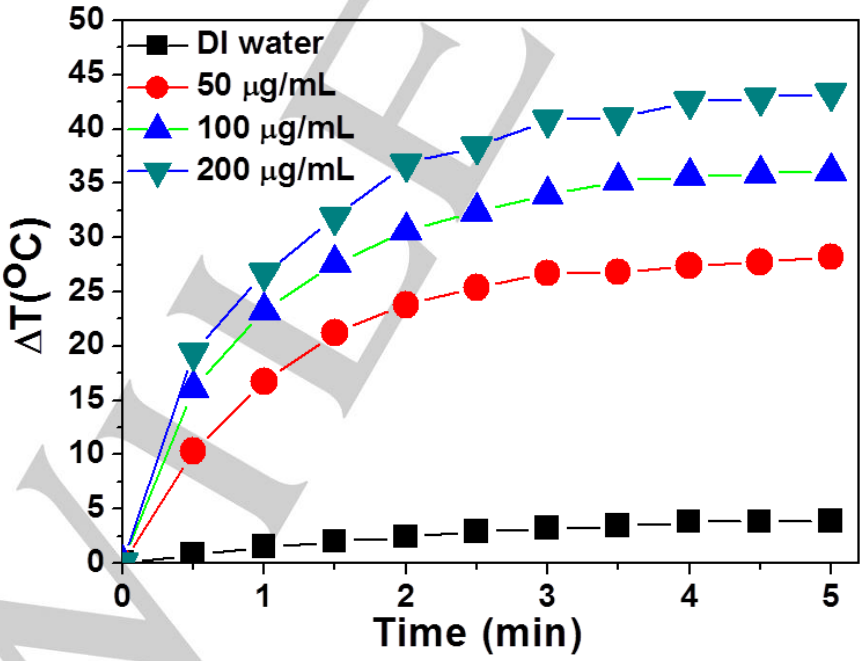

Figure S8. Temperature elevation of water and PEG-coated AMQDs aqueous solutions with different concentrations as a function of time over 5 min irradiation with an NIR laser (808 nm, 1.5 W cm^{-2}).

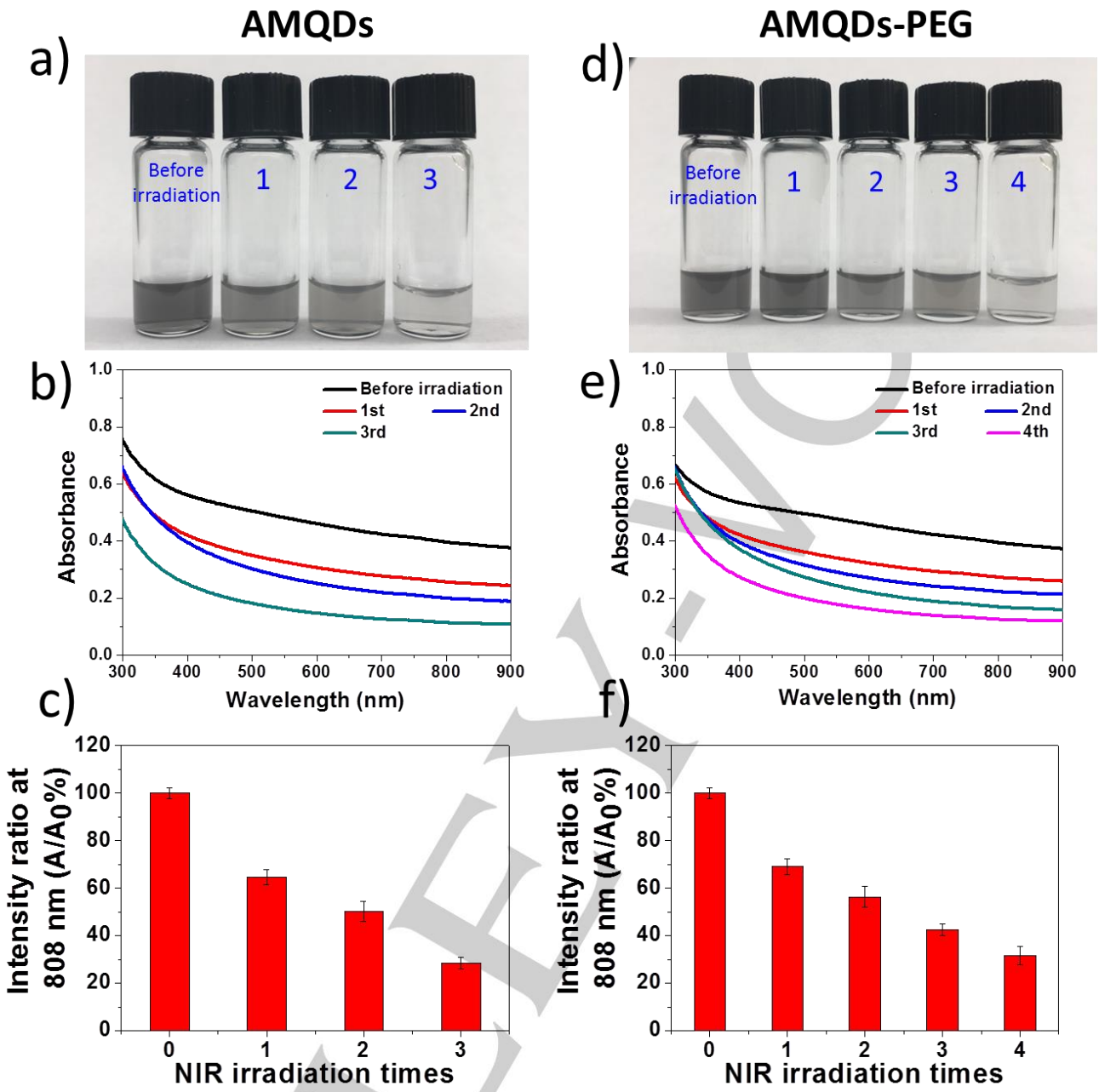

Figure S9. (a, d) Photographs, (b, e) absorbance spectra and (c, f) variation of the absorption ratios at 808 nm (A/A_0%) of as prepared AMQDs and PEG-coated AMQDs in water after different irradiation cycles.

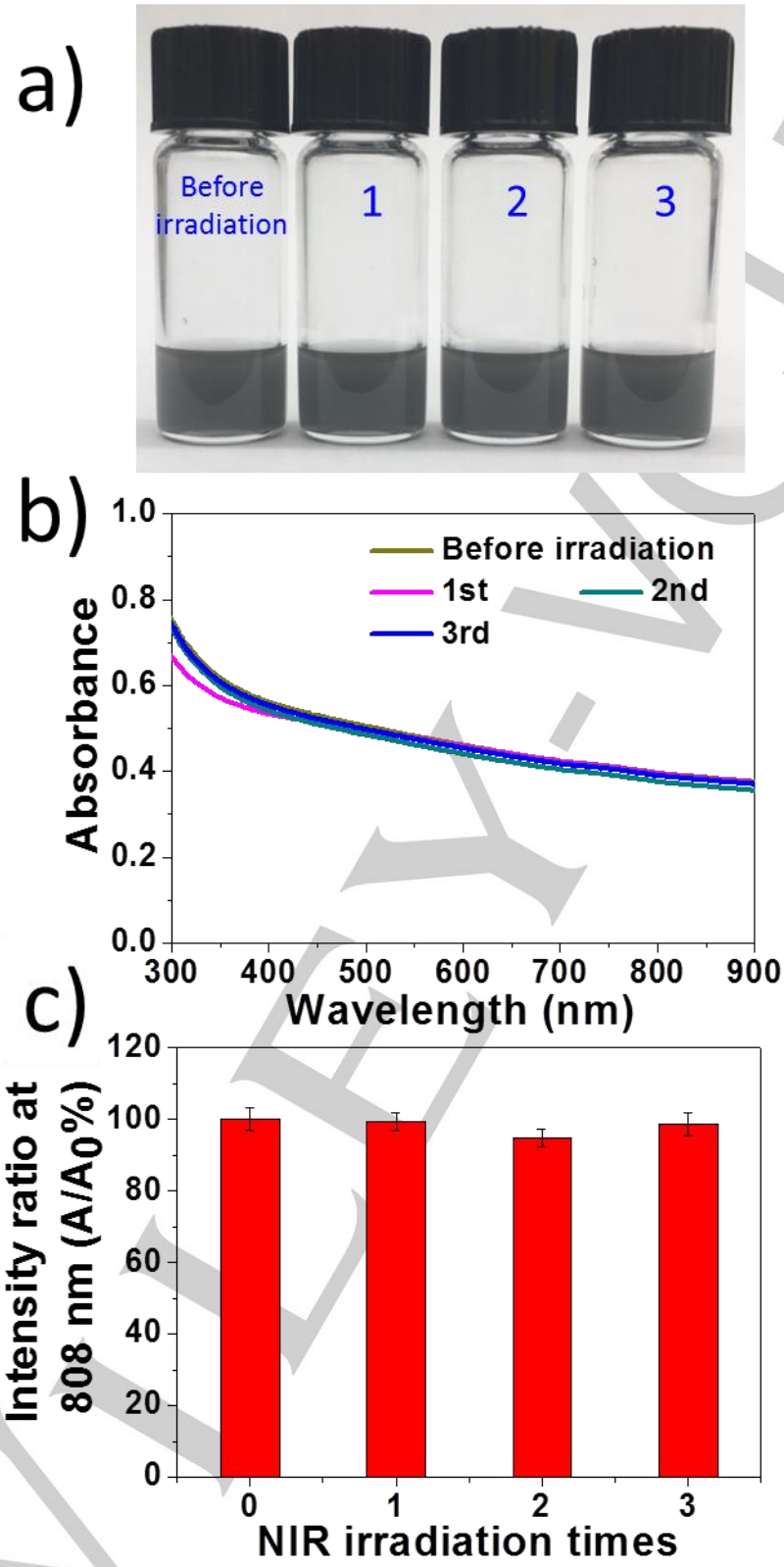

Figure S10. (a) Photographs, (b) absorbance spectra, and (c) variation of the absorption ratios at 808 nm (A/A_0%) of as-prepared AMQDs in the exfoliation solution (ethanol) after different irradiation cycles.

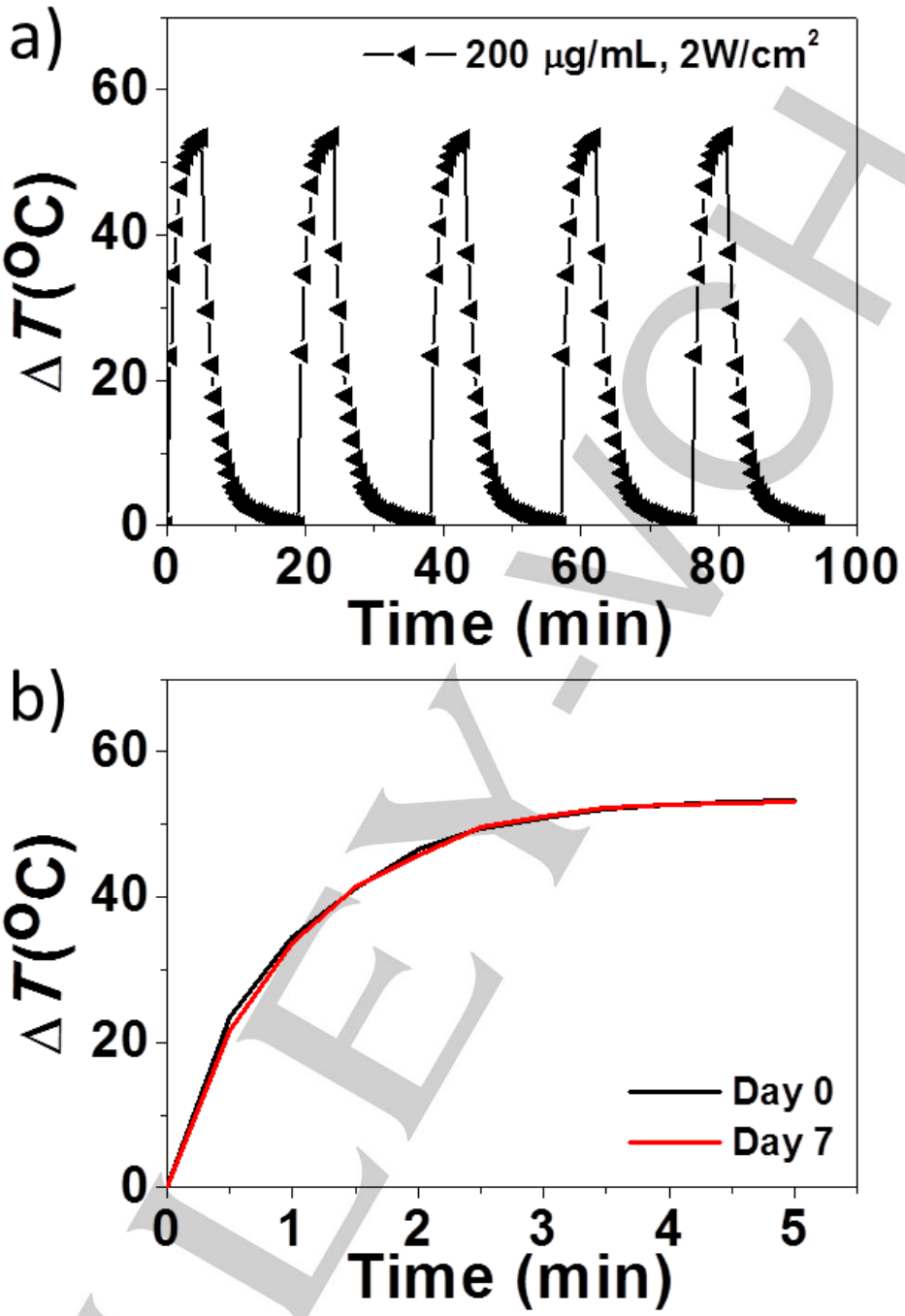

Figure S11. (a) Heating a suspension of the AMQDs for five laser on/off cycles with an 808 nm NIR laser (at power density of 2 W/cm^2) in the exfoliation solution (ethanol). (b) The change in temperature of AMQDs in the exfoliation solution (ethanol) before and after one week standing (stored at 4 °C), irradiated under an 808 nm NIR laser at power density of 2 W/cm^2.

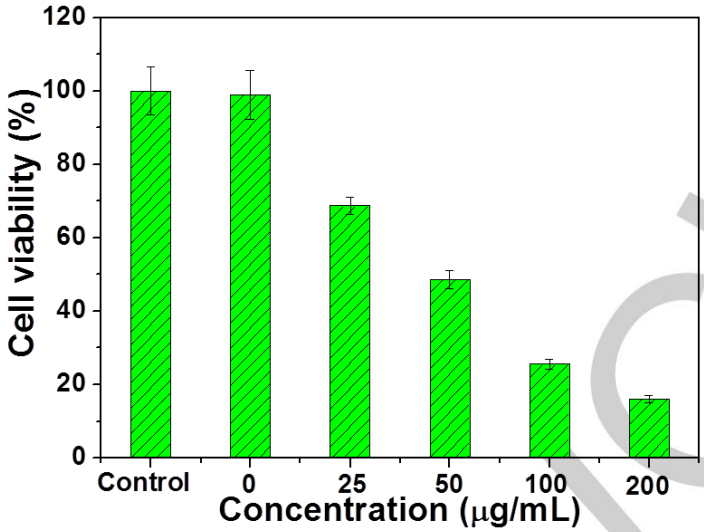

Figure S12. Viability of HeLa cells treated with different concentrations of PEG-coated AMQDs (0, 25, 50, 100, and 200 μg/mL) and irradiation with an 808-nm laser at 1.0 W cm^{-2} for 5 min. HeLa cells without any treatment were used as control.

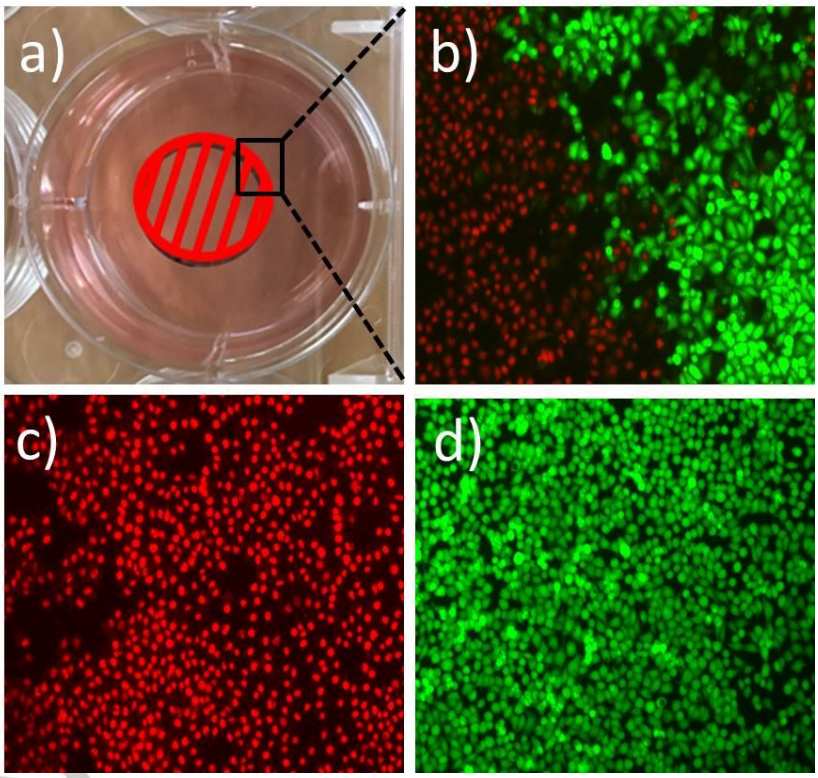

Figure S13. a) A digital photo of the HeLa cell culture dish after incubation with PEG-coated AMQDs. The red circle with a shadow shows the laser spot. b-d) Confocal images of calcein AM (green, live cells) and propidium iodide (red, dead cells) co-stained HeLa cells after laser irradiation. The magnification of confocal images is 100x.

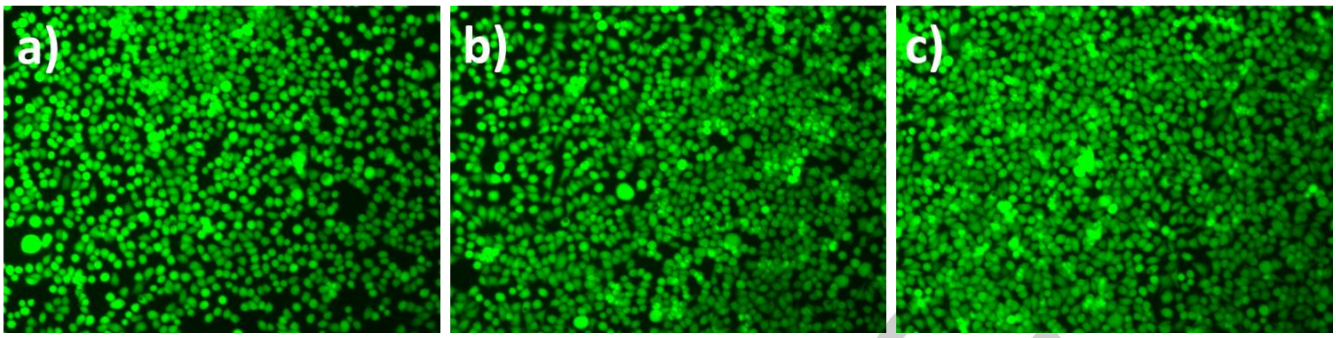

Figure S14. Confocal images of calcein AM (green, live cells) and propidium iodide (red, dead cells) co-stained MCF-7 cells with treated by a) PBS, b) only PEG-coated AMQDs, and c) only NIR. The magnification of confocal images is 100x.

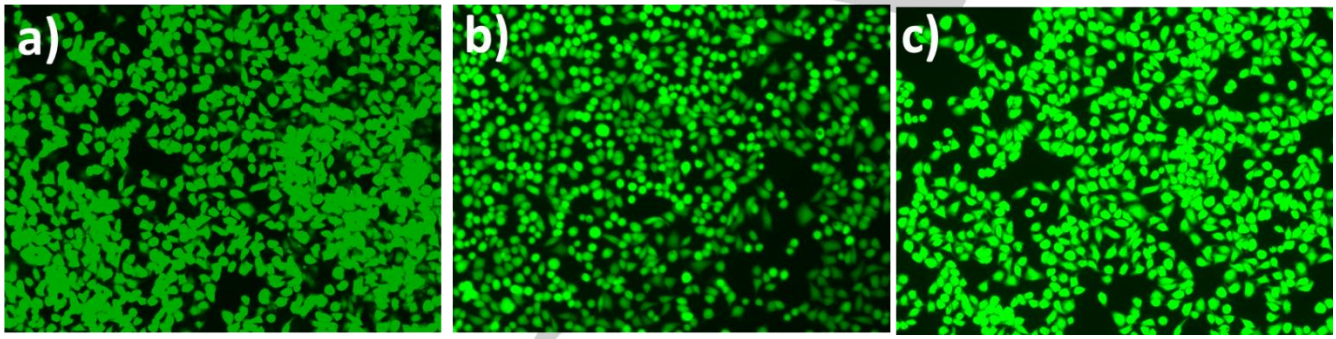

Figure S15. Confocal images of calcein AM (green, live cells) and propidium iodide (red, dead cells) co-stained HeLa cells with treated by a) PBS, b) only PEG-coated AMQDs, and c) only NIR. The magnification of confocal images is 100x.

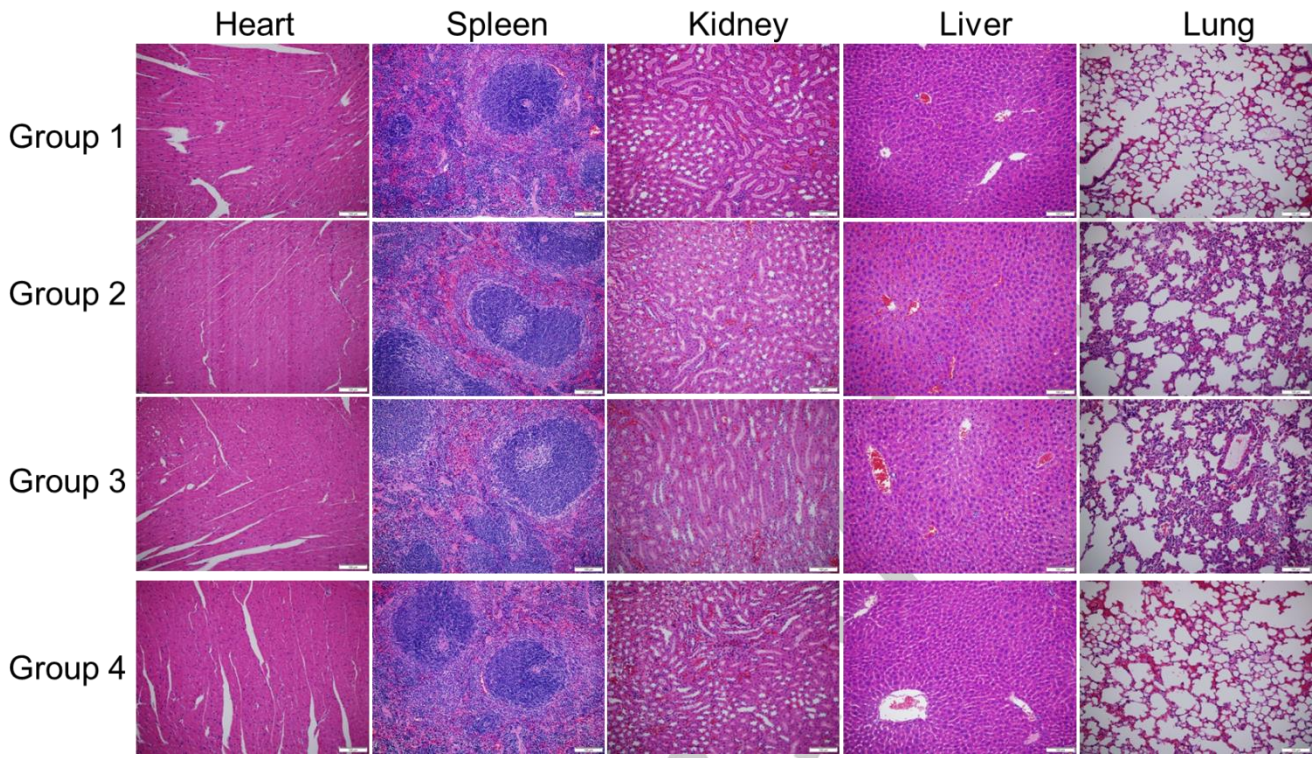

Figure S16. Histological changes in the heart, spleen, kidney, liver, and lung of mice after different treatments (Group 1: control group without treatment; Group 2: 6 mg/kg PEG-coated AMQDs via intravenous injection; Group 3: 6 mg/kg PEG-coated AMQDs via intratumoral injection; and Group 4: 6 mg/kg PEG-coated AMQDs via oral delivery). The scale bar is 500 μm.

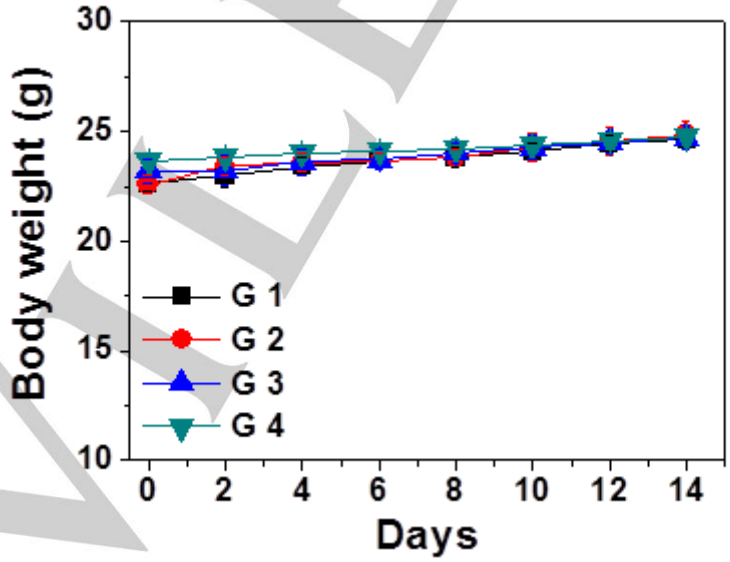

Figure S17. Body weight changes of mice in 4 groups. G1: Saline, G2: Saline + NIR (1 W cm^{-2}, 10 min), G3: PEG-coated AMQDs, and G4: PEG-coated AMQDs + NIR (1 W cm^{-2}, 10 min).

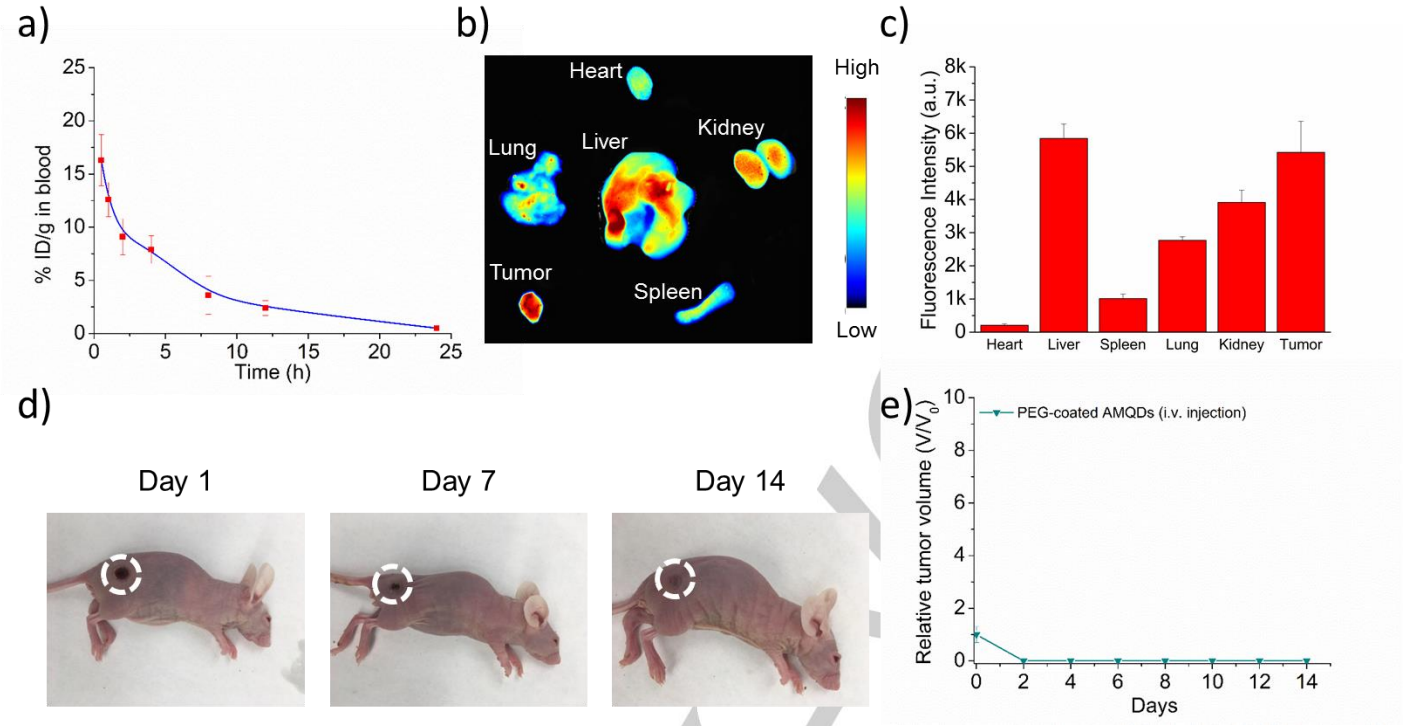

Figure S18. *In vivo* performance of PEG-coated AMQDs via i.v. injection. a) Blood circulation curve of Cy5.5-PEG-coated AMQDs determined by absorption spectra. b) NIR bio-imaging of major organs and tumors after i.v. injection at 12 h. c) Biodistribution of PEG-coated AMQDs in nude mice measured by average signals of organs and tumors from (b). d) Representative photographs of mice during the treatment period. e) Relative tumor volume in the i.v. injection group. After 12 h post-injection of 200 μL of PEG-coated AMQDs (1.2 mg/mL), the tumor sites were irradiated with an 808 nm NIR laser (2 W cm^{-2}, 10 min) on Day 0.

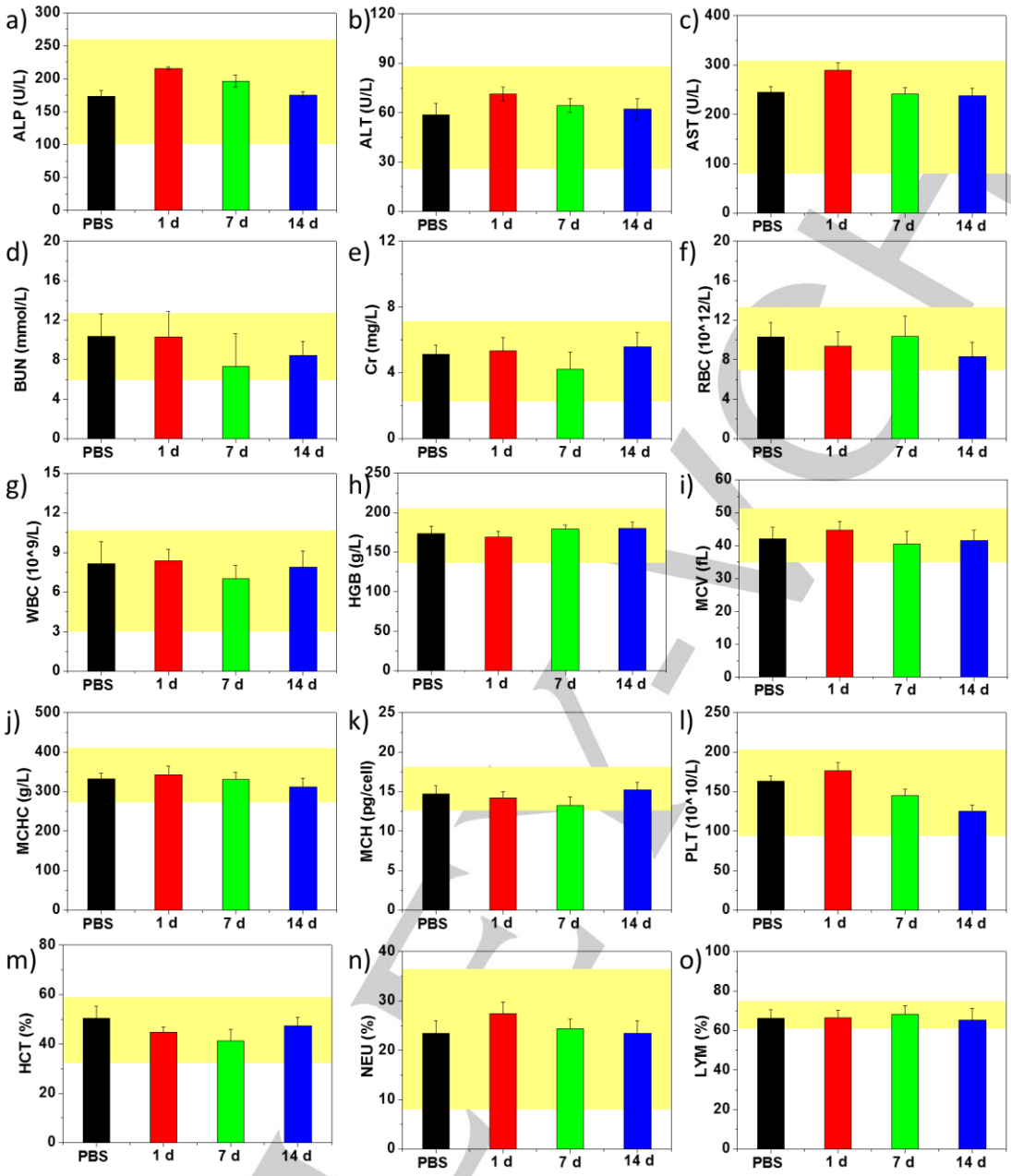

Figure S19. Serum biochemistry and complete blood panel test data of Balb/c mice treated with PEG-coated AMQDs. This data were collected at different time points following i.v. injection of 6 mg/kg PEG-coated AMQDs and PBS on Day 0. Serum biochemistry results: a) alkaline phosphatase (ALP), b) alanine aminotransferase (ALT), c) aspartate aminotransferase (AST), d) urea nitrogen (BUN) and e) creatinine (Cr) levels in the blood at different time points. Hematology results: f) Red blood cells (RBC), g) white blood cells (WBC), h) hemoglobin (HGB), i) mean corpuscular volume (MCV), j) mean corpuscular hemoglobin concentration (MCHC), k) mean corpuscular hemoglobin (MCH), l) platelet (PLT), m) hematocrit (HCT), n) Neutral Cells Percentage (NEU%) and o) Lymphocyte Percentage (LYM%) in the blood at different time points. Yellow fringe areas represent the normal reference ranges for the mice used.

Table S1 photothermal conversion efficacy of several PTT agents

PTT agents	Photothermal conversion efficacy (%)	Wavelength (nm)	References
$Cu_{2-x}Se$ nanoparticles	22	800	*Nano Lett.* 2011, *11*, 2560-2566
Cu_9S_5 nanocrystals	26	980	*ACS Nano* 2011, *5*, 9761-9771
Au nanorods	21	800	*Nano Lett.* 2011, *11*, 2560-2566
Au nanoshells	13	800	*Nano Lett.* 2011, *11*, 2560-2566
FePt nanoparticles	30	808	*Biomaterials* 2013, *34*, 1128-1134
MoS_2-CS nanosheets	24	808	*ACS Nano* 2014, *8*, 6922-6933
MoS_2-PEG nanoflakes	28	808	*Sci. Rep.* 2015, *5*, :17422
BP quantum dots	28	808	*Angew. Chem. Int. Ed.* 2015, *54*, 11526-11530
Dopamine-melanin colloidal nanospheres	40	808	*Adv. Mater.* 2013, *25*, 1353-1359
Graphene oxide	25	532	*Chem. Commun.* 2014, *50*, 14345-14348
Reduced graphene oxide	40	532	*Chem. Commun.* 2014, *50*, 14345-14348
Bi_2S_3 nanorods	28.1	808	*ACS Nano* 2015, 9, 696-707
Bi_2Se_3 nano-spherical sponges	31.1	808	*ACS Nano* 2016, 10, 9646−9658
Semimetal Sb nanorod bundles	41	808	*Biomaterials* 2015, 45, 18-26

Table S2 Raw measurements and calculations for tumor volumes of MCF-7 breast tumors in different groups of nude mice treated with G1: Saline, G2: only NIR (1W cm^{-2}, 10 min), G3: PEG-coated AMQDs only, and G4: PEG-coated AMQDs + NIR (1W cm^{-2}, 10 min)

G1	Saline					
Time		No.1	No.2	No.3	No.4	No.5
0 d	Length(mm)	7.5	8	7.9	7.1	8.1
	Width(mm)	5.3	5.1	6.4	5.7	4.9
	Weight(g)	22.3	22.5	22.6	22.1	23.6
	Volume(mm^3)	110.2533	108.8952	169.3423	120.722	101.7784
2 d	Length(mm)	8.5	8.9	8.7	8.9	9.1
	Width(mm)	6.2	6.1	7.2	6.6	6.2
	Weight(g)	22.5	23.1	22.5	22.7	24.1
	Volume(mm^3)	170.9939	173.3118	236.0275	202.888	183.0641
4 d	Length(mm)	9.3	10.5	9.8	10.2	9.4
	Width(mm)	6.9	7.1	7.8	6.9	7.2
	Weight(g)	22.9	23.1	23.4	23.2	24.4
	Volume(mm^3)	231.7179	277.003	312.0281	254.1422	255.0182
6 d	Length(mm)	9.9	11.2	10.1	10.9	10.2
	Width(mm)	7.5	7.6	8.7	7.8	7.3
	Weight(g)	23.1	23.4	23.6	23.7	24.5
	Volume(mm^3)	291.4313	338.5506	400.0721	347.0516	284.462
8 d	Length(mm)	10.5	11.3	10.6	10.4	10.2
	Width(mm)	8.4	8.3	9.8	8.5	8.8
	Weight(g)	23.3	23.5	23.7	23.6	24.9
	Volume(mm^3)	387.7272	407.3925	532.7659	393.2327	413.3747
10 d	Length(mm)	11.7	11.9	11.5	11.8	11.3
	Width(mm)	9.2	8.9	10.6	9.3	9.7
	Weight(g)	23.6	24.1	23.8	23.9	25
	Volume(mm^3)	518.2507	493.2935	676.2199	534.1046	556.4169
12 d	Length(mm)	12.5	12.9	12.9	12.4	12.7
	Width(mm)	10.2	10.1	11.5	10.3	10.2
	Weight(g)	23.9	24.2	24.3	24.5	25.4
	Volume(mm^3)	680.595	688.6695	892.8198	688.4534	691.4845
14 d	Length(mm)	13.1	13.8	13.9	13.3	13.5
	Width(mm)	10.8	10.7	12.1	10.8	10.7
	Weight(g)	24.1	24.3	24.5	24.5	25.6
	Volume(mm^3)	799.645	826.8468	1065.035	811.8533	808.8719

G2	Only NIR					
Time		No.1	No.2	No.3	No.4	No.5
0 d	Length(mm)	7.2	8.5	7.3	8.1	8.2
	Width(mm)	5.4	6.1	5.7	5.2	5
	Weight(g)	22.4	22.1	22.5	23.6	22.3
	Volume(mm^3)	109.8749	165.5225	124.1226	114.6226	107.2833
2 d	Length(mm)	8.3	8.9	8.5	8.4	8.8
	Width(mm)	6.2	7.1	6.4	6.7	6.5
	Weight(g)	22.7	23.3	23.5	24.4	23.3
	Volume(mm^3)	166.9705	234.793	182.2037	197.3364	194.5753
4 d	Length(mm)	9.3	10.4	9.1	9.5	9.3
	Width(mm)	6.8	7.9	7.2	6.9	7
	Weight(g)	23.1	23.2	23.5	24.6	23.4
	Volume(mm^3)	225.0501	339.6768	246.8794	236.7011	238.483
6 d	Length(mm)	10.2	11.2	10.3	9.8	10.1
	Width(mm)	7.3	8.7	7.2	7.4	7.5
	Weight(g)	23.3	23.5	23.1	24.6	23.7
	Volume(mm^3)	284.462	443.6443	279.4349	280.8458	297.3188
8 d	Length(mm)	11	12.4	10.7	10.3	10.6
	Width(mm)	8.3	9.6	8.6	8.7	8.5
	Weight(g)	23.3	23.5	23.7	24.6	23.9
	Volume(mm^3)	396.5768	598.057	414.1513	407.9943	400.7948
10 d	Length(mm)	12.1	13.3	11.8	11.5	12.1
	Width(mm)	9.3	10.4	9.2	9.5	9.4
	Weight(g)	23.6	24.1	23.8	25.9	24
	Volume(mm^3)	547.6835	752.8297	522.6802	543.1546	559.525
12 d	Length(mm)	13.2	14.1	12.8	13.2	13
	Width(mm)	10.2	11.8	9.8	10.3	10
	Weight(g)	23.6	24.3	24.4	26.1	24.4
	Volume(mm^3)	718.7083	1027.452	643.3399	732.8697	680.3333
14 d	Length(mm)	13.5	14.7	13.8	13.5	13.7
	Width(mm)	11	12.1	10.3	10.9	11.1
	Weight(g)	24.3	24.1	24.6	26.3	25
	Volume(mm^3)	854.865	1126.332	766.182	839.3927	883.3746

G3	Only PEG-coated AMQDs					
Time		No.1	No.2	No.3	No.4	No.5
0 d	Length(mm)	7.1	8.3	7.4	7.6	8.1
	Width(mm)	5.5	5.7	6.1	5.9	5.3
	Weight(g)	24.1	23.1	23.1	23.7	22.1
	Volume(mm^3)	112.3989	141.1257	144.1019	138.451	119.0735
2 d	Length(mm)	9.2	8.9	8.8	8.3	9.4
	Width(mm)	6.3	6.1	7.2	6.7	7.5
	Weight(g)	24.4	23.2	22.5	23.7	22.2
	Volume(mm^3)	191.0941	173.3118	238.7405	194.9872	276.7125
4 d	Length(mm)	9.5	9.8	9.7	9.1	9.8
	Width(mm)	7.1	7.5	7.9	7.2	8.4
	Weight(g)	24.6	23.4	23.4	24.1	22.5
	Volume(mm^3)	250.6217	288.4875	316.814	246.8794	361.8787
6 d	Length(mm)	10.9	11.2	10.6	11.4	10.8
	Width(mm)	7.7	7.4	8.1	7.9	9.2
	Weight(g)	24.6	23.7	23.6	24	22.7
	Volume(mm^3)	338.2099	320.9666	363.9605	372.3381	478.3853
8 d	Length(mm)	11.4	11.7	11.2	11.6	12.5
	Width(mm)	8.6	8.2	8.8	8.3	9.9
	Weight(g)	24.9	24	23.9	24.3	23
	Volume(mm^3)	441.2454	411.7105	453.9017	418.2082	641.1488
10 d	Length(mm)	12.1	11.5	11.7	11.4	13.2
	Width(mm)	9.1	8.8	9.2	9.1	10.3
	Weight(g)	25.1	24.5	23.8	24.5	23.3
	Volume(mm^3)	524.3805	466.0597	518.2507	494.0445	732.8697
12 d	Length(mm)	12.4	12.2	13	12.3	13.5
	Width(mm)	11.1	11.4	11.2	11	11.7
	Weight(g)	25.2	24.9	24.3	24.7	23.4
	Volume(mm^3)	799.5508	829.7513	853.4101	778.877	967.1279
14 d	Length(mm)	13.2	13.1	13.2	13.7	14.3
	Width(mm)	10.3	10.8	11.2	12.1	12.1
	Weight(g)	25.3	25.3	24.8	24.9	23.4
	Volume(mm^3)	732.8697	799.645	866.5395	1049.711	1095.684

G4	PEG-coated AMQDs + NIR					
Time		No.1	No.2	No.3	No.4	No.5
0 d	Length(mm)	6.8	8.6	7.8	8	8.1
	Width(mm)	5.1	5.5	6.2	6	5.4
	Weight(g)	23.4	24.1	23.4	24.1	23.4
	Volume(mm^3)	92.56092	136.1452	156.9121	150.72	123.6092
2 d	Length(mm)	0	0	0	0	0
	Width(mm)	0	0	0	0	0
	Weight(g)	23.5	24.3	23.6	24.3	23.5
	Volume(mm^3)	0	0	0	0	0
4 d	Length(mm)	0	0	0	0	0
	Width(mm)	0	0	0	0	0
	Weight(g)	23.7	24.5	23.8	24.4	23.7
	Volume(mm^3)	0	0	0	0	0
6 d	Length(mm)	0	0	0	0	0
	Width(mm)	0	0	0	0	0
	Weight(g)	23.8	24.6	23.9	24.5	23.8
	Volume(mm^3)	0	0	0	0	0
8 d	Length(mm)	0	0	0	0	0
	Width(mm)	0	0	0	0	0
	Weight(g)	23.8	24.8	24	24.6	23.9
	Volume(mm^3)	0	0	0	0	0
10 d	Length(mm)	0	0	0	0	0
	Width(mm)	0	0	0	0	0
	Weight(g)	24	24.9	24.2	24.8	24.1
	Volume(mm^3)	0	0	0	0	0
12 d	Length(mm)	0	0	0	0	0
	Width(mm)	0	0	0	0	0
	Weight(g)	24.1	25.1	24.5	24.9	24.2
	Volume(mm^3)	0	0	0	0	0
14 d	Length(mm)	0	0	0	0	0
	Width(mm)	0	0	0	0	0
	Weight(g)	24.4	25.2	24.7	25	24.4
	Volume(mm^3)	0	0	0	0	0

References

[1] J. T. Robinson, S. M. Tabakman, Y. Liang, H. Wang, H. S. Casalongue, D. Vinh, H. Dai, *J Am Chem Soc* **2011**, *133*, 6825-6831.

[2] Z. Sun, H. Xie, S. Tang, X.-F. Yu, Z. Guo, J. Shao, H. Zhang, H. Huang, H. Wang, P. K. Chu, *Angew. Chem. Int. Ed.* **2015**, *54*, 11526-11530.

[3] a) D. K. Roper, W. Ahn, M. Hoepfner, *J. Phys. Chem. C* **2007**, *111*, 3636-3641; b) Y. Liu, K. Ai, J. Liu, M. Deng, Y. He, L. Lu, *Adv. Mater.* **2013**, *25*, 1353-1359; c) W. Li, P. Rong, K. Yang, P. Huang, K. Sun, X. Chen, *Biomaterials* **2015**, *45*, 18-26.